FAMILY OF STEPPED-FREQUENCY LFM TRAINS WITH LOW AUTOCORRELATION SIDELOBES

Dmitry Chebanov
Ph.D. Program in Computer Science
The Graduate Center of CUNY
365 Fifth Avenue
New York, NY 10016, USA
email: chebanov@cs.ccny.cuny.edu

Irina Gladkova† and John Weber‡
NOAA-CREST
City College of New York
138th Street and Convent Avenue
New York, NY 10031, USA
email: †gladkova@cs.ccny.cuny.edu,‡weber@cs.ccny.cuny.edu

ABSTRACT
Modern radars transmit pulses with wide overall bandwidth to achieve high range resolution. In the case, when such wideband pulses are undesirable due to the expensive hardware needed to support the wide instantaneous bandwidth, frequency-stepping technique that allows the transmission of extremely wideband waveforms by a radar with a relatively small instantaneous bandwidth is used.

In this paper we consider a new family of stepped-frequency waveforms designed for the purposes of high range resolution. We show that a suitable choice of waveform's parameters leads to the essential suppression of its autocorrelation function (ACF) sidelobes. We perform analysis of the set of parameter values that provide sidelobe suppression below some predetermined level.

KEY WORDS
Radar, signal processing, autocorrelation function, stepped-frequency LFM train, time sidelobes

1 Introduction

A stepped-frequency waveform is a collection of short narrowband pulses separated by time intervals that are sufficient to receive scattering echoes from the targets located at some range of interest. Once the echoes from all the pulses have been received, they, then, are processed in the receiver collectively.

The center frequencies of the pulses are shifted with respect to each other, as shown, for example, in Figure 1 where a stepped-frequency LFM pulse train with a constant frequency step between consecutive pulses is schematically depicted. The presence of the frequency shifts allows one to transmit stepped-frequency waveforms with, virtually, arbitrary overall bandwidth by a radar with a quite small instantaneous bandwidth. This fact is regarded [1, 2] as the main advantage of these waveforms and makes them useful in high range resolution radars.

Waveforms with wide overall bandwidth created synthetically were introduced in the 1960's [3]. As pointed out in [4], the S-band Tradex radar (located on the U.S. Army's Kwajelein Missile Range facility) implemented waveforms of this type in 1974 and experiments using the Aegis SPY-1 radar, the Patriot radar, and RSTER have been performed since then.

As usually happens, stepped-frequency waveforms have some disadvantages. Among them, the appearance of relatively high undesirable spikes (range sidelobes and grating lobes) in the profile of the magnitude of the waveform's ACF is thought to be the main one. It turns out, however, that, if both the instantaneous bandwidth and the total processing bandwidth of a radar are given, right choice of the frequency shifts between pulses, the number of pulses to be processed and/or their amplitudes leads to essential reduction of delay sidelobes. Indeed, any changes in the values of the parameters mentioned above cause reshaping the waveform's spectrum, introducing frequency weighting – the main approach for achieving time sidelobes suppression.

Recent publications [4-7] have addressed the issue of high ACF sidelobes in stepped-frequency LFM trains. Papers [5, 6] have discussed different approaches leading to either acceptable suppression or complete elimination of the grating lobes by appropriate choice of the constant frequency step. Publications [4, 7] claim that it is possible to design a resulting waveform whose spectrum would approximate one of the known weighting functions. It can be done either by increasing the amplitude of the pulses [7] or by staggering the uniform stepping in the frequency domain [4]. In both cases, the number of pulses constituting the train controls the quality of such approximation. As the result, desired suppression of time sidelobes can be achieved.

In this paper we propose a new systematic approach for designing stepped-frequency LFM pulse trains producing the ACF whose peaks are lowered below some predetermined level. It is based on the usage of variable frequency steps that are introduced by means of specific relationships between the positions of the center frequencies of the pulses. Our approach (which is analytical rather than numerical) advantages from the fact that the ACF of the resulting waveform is available in the closed form. This gives us possibility to search for waveforms with a desired threshold level by analyzing the set of their parameter values. Suitable selection of the parameters allows us to design a variety of LFM trains with excellent ACF profiles.

2 Non-uniform Stepped-Frequency Train of LFM Pulses

In this paper we study the performance of compound waveforms we define as follows.

We start with a traditional coherent stepped-frequency train $s(t)$ of N LFM pulses, depicted in Figure 1. Its complex envelope is given by (see [2, 5])

$$s(t) = \frac{1}{\sqrt{N}}\, e^{j\pi k_N t^2} \sum_{n=0}^{N-1} s_p(t - nt_r), \qquad (1)$$

where

$$s_p(t) = \frac{1}{\sqrt{t_p}}\, \mathrm{rect}\left(\frac{t}{t_p}\right) e^{j\pi k_p t^2} \qquad (2)$$

is an LFM pulse of duration t_p and t_r is the time repetition interval which is assumed to be chosen such that the duty cycle, t_r/t_p, is greater than 2. We also assume that the frequency slopes k_N and k_p are positive. The first factors in both formulas (1) and (2) are added to maintain the unit energy of waveforms $s(t)$ and $s_p(t)$, respectively.

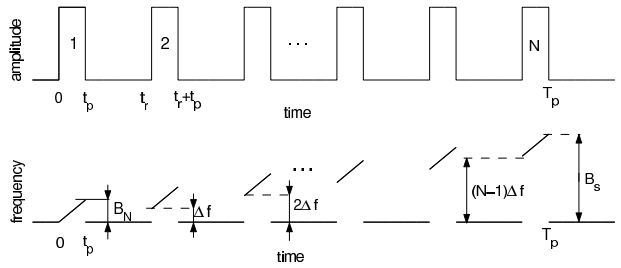

Figure 1. Stepped-frequency LFM pulse train $s(t)$ with constant frequency step Δf.

We will denote the bandwidth of each subpulse, $\widetilde{s}_n(t) = e^{j\pi k_N t^2} s_p(t - nt_r)$, in train (1) by B_N, that is $B_N = (k_N + k_p)t_p > 0$. Note that the presence of the second term, $e^{j\pi k_N t^2}$, in the factorization (1) creates a constant frequency step $\Delta f = k_N t_r (0 < \Delta f \le B_N)$ between the center frequencies of consecutive subpulses in the train $s(t)$ (see Figure 1). This leads to the essential broadening of the waveform's total bandwidth which becomes equal to $B_s = B_N + (N-1)\Delta f$. The total time duration of $s(t)$ is $T_p = (N-1)t_r + t_p$.

Next, we use the waveform $s(t)$ as a single component to create a uniform train of M subpulses $u_p(t) = s(t)$ (see Figure 2):

$$u_M(t) = \frac{1}{\sqrt{M}} \sum_{m=0}^{M-1} u_p(t - mT_r) \qquad (3)$$

with the pulse repetition interval $T_r > 2T_p$.

Finally, we add an LFM with the frequency slope k_M ($k_M > 0, k_M \neq k_N + k_p$) to the entire train (3) (see

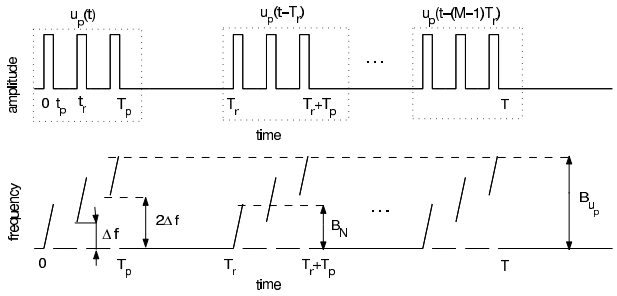

Figure 2. Non-uniform stepped-frequency pulse train $u_M(t)$.

Figure 3):

$$u(t) = u_M(t)\, e^{j\pi k_M t^2} = \frac{1}{\sqrt{MN}}\, e^{j\pi k_M t^2} \times \sum_{m=0}^{M-1} e^{j\pi k_N (t - mT_r)^2} \sum_{n=0}^{N-1} s_p(t - nt_r - mT_r). \qquad (4)$$

As the result, we obtain a non-uniform train of NM pulses that can be divided into M portions $u^{(1)}(t)$, $u^{(2)}(t)$, $\ldots$, $u^{(M)}(t)$, where

$$u^{(i)}(t) = e^{j\pi k_M t^2} u_p(t - (i-1)T_r)$$

with $t \in [(i-1)T_r, (i-1)T_r + T_p],\ i = 1, 2, \ldots, M$.

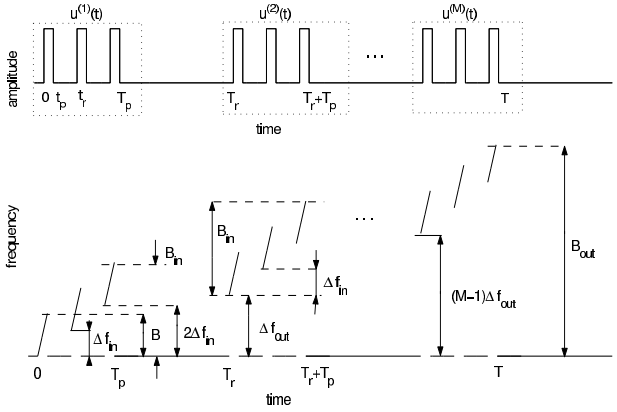

Figure 3. Time-energy (top) and time-frequency (bottom) distributions of non-uniform LFM pulse train $u(t)$ with nonconstant frequency step.

Each such a portion $u^{(i)}(t)$ of the "outer" train $u(t)$ is an "inner" periodic stepped-frequency train of N pulses, each of duration t_p, with the ultimate bandwidth

$$B = B_N + k_M t_P = (k_p + k_N + k_M)t_p > 0. \qquad (5)$$

After adding the LFM in (4), the "inner" frequency step between consecutive pulses in $u^{(i)}(t)$ becomes

$$\Delta f_{in} = \Delta f + k_M t_r = (k_N + k_M)t_r > 0. \qquad (6)$$

We suppose that there would be either some frequency overlap between neighbor components of $u^{(i)}(t)$ ($\Delta f_{in} < B$) or the uniform energy distribution over the frequency band B_{in} of $u^{(i)}(t)$ ($\Delta f_{in} = B$), which is equal to $B_{in} = B + (N-1)\Delta f_{in} > 0$. We recall that the total duration of $u^{(i)}(t)$ ($i = 1, 2, \ldots, M$) is T_p.

At the same time, "inner" trains $u^{(1)}(t)$, $u^{(2)}(t)$, $\ldots, u^{(M)}(t)$ form the "outer" train $u(t)$. In the time-frequency domain, the band of each train $u^{(i)}(t)$ ($i = 2, 3, \ldots, M$) is shifted with respect to the band of $u^{(i-1)}(t)$ by the constant frequency step

$$\triangle f_{out} = k_M T_r > 0. \tag{7}$$

Again, we suppose that $\Delta f_{out} \leq B_{in}$. Finally, we note that the total time duration of $u(t)$ is $T = T_p + (M-1)T_r = t_p + (N-1)t_r + (M-1)T_r$ and the combined frequency deviation of $u(t)$ is $B_{out} = B_{in} + (M-1)\Delta f_{out} = B + (N-1)\Delta f_{in} + (M-1)\Delta f_{out}$.

3 Autocorrelation Function of Waveform (4)

It is well-known (see, for example, [2]) that the ACF of a pulse train with $t_r \geq 2t_p$ is a collection of nonoverlapping envelopes distributed along the time-delay axis. Among those envelopes, the central one, corresponding to the time-delay interval $|\tau| \leq t_p$ and containing the main lobe, has the most practical importance, since, primarily, its shape evaluates the quality of radar measurements. In this section, we derive the analytical representation for the central envelope of the ACF $R_u(\tau)$ of $u(t)$ and analyze its shape.

It is shown in [5, 6] that, for $|\tau| \leq t_p$, the magnitude of the ACF $R_s(\tau)$ of "simple" stepped-frequency train (1) is the two-term product:

$$|R_s(\tau)| = |R_{\widetilde{s}_n}(\tau)| \cdot \left| \frac{\sin(N\pi\tau\triangle f)}{N\sin(\pi\tau\triangle f)} \right|. \tag{8}$$

The first factor in (8) is the magnitude of the ACF of a single subpulse $\widetilde{s}_n(t)$ constituting the train (1), whereas the second factor is a periodic sinc function which appears due to the uniformity of $s(t)$.

We recall from the previous section that waveform $u(t)$ can be thought as a stepped-frequency train of M subpulses $u^{(i)}(t)$ with the constant frequency step Δf_{out}. Hence, similar to (8), we obtain, for $|\tau| \leq T_p$, that $|R_u(\tau)| = |R_{u^{(i)}}(\tau)| \cdot |R_3(\tau)|$, where

$$|R_3(\tau)| = \left| \frac{\sin(M\pi\tau\Delta f_{out})}{M\sin(\pi\tau\Delta f_{out})} \right| \tag{9}$$

and $|R_{u^{(i)}}(\tau)|$ represents the magnitude of the ACF of any subpulse $u^{(i)}(t)$. Since all the $|R_{u^{(i)}}(\tau)|$ ($i = 1, 2, \ldots, M$) are the same, we write, without loss of generality, $|R_{u^{(1)}}(\tau)|$ instead of $|R_{u^{(i)}}(\tau)|$ in our derivation below.

Now we note that $u^{(1)}(t)$ is itself a stepped-frequency train of N components $\widehat{s}_n(t) = e^{j\pi k_M t^2}\widetilde{s}_n(t)$ with the constant frequency step Δf_{in}. So, again by analogy with (8), we have $|R_{u^{(1)}}(\tau)| = |R_1(\tau)| \cdot |R_2(\tau)|$, where $|\tau| \leq t_p$,

$$|R_1(\tau)| = |(1 - |\tau|/t_p)\,\mathrm{sinc}\,(B\tau\,(1 - |\tau|/t_p))| \tag{10}$$

is the magnitude of the ACF of any single subpulse $\widehat{s}_n(t)$ in the component train $u^{(1)}(t)$, and

$$|R_2(\tau)| = \left| \frac{\sin(N\pi\tau\Delta f_{in})}{N\sin(\pi\tau\Delta f_{in})} \right|. \tag{11}$$

Finally, based on the above discussion, we conclude that, for $|\tau| \leq t_p$,

$$|R_{\widetilde{u}}(\tau)| = |R_1(\tau)| \cdot |R_2(\tau)| \cdot |R_3(\tau)|, \tag{12}$$

where the factors in the right-hand side are defined by formulas (10), (11), and (9) and the quantities $B, \Delta f_{in}$, and Δf_{out} they contain are given by relations (5), (6), and (7), respectively.

Thus, the ACF of proposed here waveform $u(t)$ is the three-term product (12), where the first factor represents the ACF of any single subpulse forming the train and $|R_2(\tau)|$ and $|R_3(\tau)|$ are periodic sinc functions that appear due to the "inner" and "outer" trains described in the previous section. Although the structure of $|R_u(\tau)|$ is more complicated than that one for the ACF of a traditional stepped-frequency LFM train (shown in (8)), each term in the product (12) admits a simple geometric interpretation (see Figure 4 for details). Evidently, the relationship between the shapes of $|R_1(\tau)|, |R_2(\tau)|$, and $|R_3(\tau)|$ determines the $|R_u(\tau)|$'s profile and, as consequence, the height of the $|R_u(\tau)|$'s sidelobes.

Depending on their sources and locations, the sidelobes of $|R_u(\tau)|$ can be classified into groups in the fashion similar to the classification of the $|R_s(\tau)|$'s sidelobes. Namely, we distinguish grating lobes (that are caused by the presence of two last factors in (12) and located near the points of their maxima, i.e.

$$\tau_p^{\text{gr_in}} = \frac{p}{\Delta f_{in}} \quad \text{and} \quad \tau_q^{\text{gr_out}} = \frac{q}{\Delta f_{out}}$$

with $p = 1, 2, \ldots, \lfloor t_p \Delta f_{in} \rfloor$ and $q = 1, 2, \ldots, \lfloor t_p \Delta f_{out} \rfloor$), a few range sidelobes surrounding the main lobe, etc.

Figure 4 illustrates a typical profile of $|R_u(\tau)|$ with indication of two important groups (range and grating lobes) of time sidelobes. (Since the magnitude of the ACF is symmetric with respect to the origin, in all the figures presented here, we show the shape of its central envelope for the delay interval $0 \leq \tau \leq 1$ only.) These groups would normally contain all the high sidelobes of $|R_u(\tau)|$. We denote two first (out of total four) range sidelobes near the main lobe of $|R_u(\tau)|$ by r_1 and r_2. The g_is (i=1,2,..., 7) indicate all the grating lobes presented in the ACF's profile. Note that most of the grating lobes are located not exactly at the maxima of $|R_i(\tau)|(i = 2, 3)$, but at their close vicinity. The lobes g_2, g_4, and g_6 are caused by each of two last factors in (12), while g_1, g_3, g_5, and g_7 arise due to the third one only.

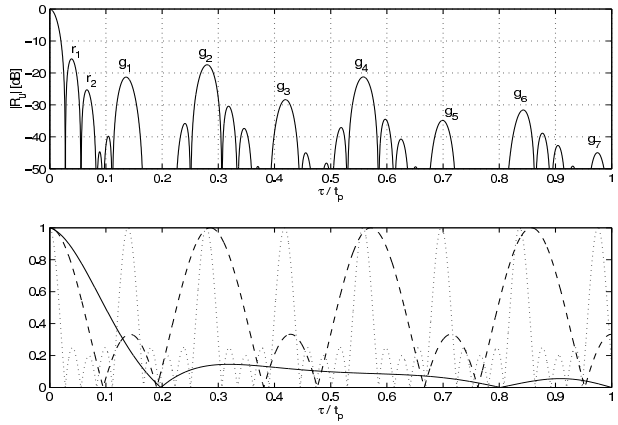

Figure 4. Top: the magnitude of the ACF of $u(t)$ with $N = 3, M = 5, \Delta f_{in} t_p = 3.5, \Delta f_{out} t_p = 7.175$, and $B t_p = 6.3$ (zoom on the interval $0 \le \tau/t_p \le 1$). Bottom: the relationship between $|R_1(\tau)|$ (solid), $|R_2(\tau)|$ (dashed), and $|R_3(\tau)|$ (dotted).

4 Suppression of Autocorrelation Sidelobes in Train (4)

As can be noticed from Figure 4, the ACF produced by train (4) contains, in general, a number of relatively high peaks essentially reducing the waveform's resolution capabilities. Analyzing the shape of the factors $|R_i(\tau)|(i = 1, 2, 3)$, however, one can observe that it is possible to choose the $u(t)$'s parameters such that the values of two of those three factors would be relatively small at the points where the third one attains its largest values. Hence, multiplying the factors altogether should result in the ACF that takes on small values along the time-delay axis. Furthermore, a quite simple analytical representation (12) for $|R_u(\tau)|$ and relatively small number of the waveform's parameters make it possible to perform a systematic search for waveforms whose ACF sidelobes lowered below a desired level. Below we describe our approach and present results we have obtained.

4.1 Preliminary Comments

In this subsection we describe briefly the set of assumptions and restrictions we have made while analyzing the shape of $|R_u(\tau)|$.

First, we assume that the total number $K = NM$ of pulses in the train (4) is given and form the set Λ of all possible two-term factorizations of K with both factors greater than unity, i.e. $\Lambda = \{(n, m) : n, m \in \mathbb{Z}^+, n, m \ge 1, n \cdot m = K\}$. Then, for each pair $(n, m) \in \Lambda$, we let $N = n, M = m$ and look for values of the remaining parameters (i.e. $B, \Delta f_{in}, \Delta f_{out}$, and t_p) that would guarantee a low level of $u(t)$'s time sidelobes.

In what follows, we restrict the range of the parameters under consideration by the following set of conditions:

i) We recall from section 2 that $\Delta f_{in} \le B$ and $\Delta f_{out} \le B_{in}$. The last is equivalent to $\Delta f_{out}/\Delta f_{in} \le B/\Delta f_{in} + N - 1$.

ii) We require that $|R_u(\tau)|(0 < \tau < t_p)$ would have at least one grating lobe caused by each of the terms $|R_2(\tau)|$ and $|R_3(\tau)|$. It can be done, if both Δf_{in} and Δf_{out} are greater than unity.

iii) We denote the first (counting from the origin) positive null of $|R_i(\tau)|$ by $\tau_i^{\text{null}}(i = 1, 2, 3)$. It can be noticed from (10), (11), and (9) that $\tau_1^{\text{null}} \approx 1/B, \tau_2^{\text{null}} = 1/(N\Delta f_{in})$, and $\tau_3^{\text{null}} = 1/(M\Delta f_{out})$. Now we suppose that the first null τ^{null} of $|R_u(\tau)|$ (that manages the ACF main lobe width – one of most important resolution characteristics) would be originated by the first null of either $|R_2(\tau)|$ or $|R_3(\tau)|$, that is $\tau^{\text{null}} = \min\{\tau_2^{\text{null}}, \tau_3^{\text{null}}\}$. This fact implies that $\tau_1^{\text{null}} \ge \min\{\tau_2^{\text{null}}, \tau_3^{\text{null}}\}$. In other words, we obtain that $B/\Delta f_{in} \le N$, if $\Delta f_{out}/\Delta f_{in} \le N/M$, and $B/\Delta f_{out} \le M$, otherwise.

We remark here that the first (from the main lobe) grating lobe of $|R_u(\tau)|$ arises near the point $\tau_{\text{min}}^{\text{gr}} = \min\{\tau_1^{\text{gr_in}}, \tau_1^{\text{gr_out}}\} = \min\{1/\Delta f_{in}, 1/\Delta f_{out}\}$. That is why below we refer to the intervals $I_{\text{r}} = (\tau^{\text{null}}, \tau_{\text{min}}^{\text{gr}})$ and $I_{\text{gr}} = [\tau_{\text{min}}^{\text{gr}}, t_p)$ as of range sidelobes and grating lobes regions, respectively.

iv) Note that if one seeks to push all the sidelobes, appearing in the grating lobes region, below some predetermined level ϵ (here ϵ is some small, a priori chosen, value defining the desired level of sidelobes suppression), then, generally speaking, only a few (if any) time sidelobes, belonging to a portion of I_{gr}, should be pushed down in order to satisfy this desideratum. Indeed, since all the factors in (12) do not exceed 1 and, for any $\tau > 0$, the $|R_1(\tau)|$ admits an upper estimate

$$|R_1(\tau)| = \frac{|\sin(\pi B\tau(1 - |\tau|/t_p))|}{\pi B\tau} \le \frac{1}{\pi B\tau}, \qquad (13)$$

we conclude that the inequality $|R_u(\tau)| \le \epsilon$ will be automatically fulfilled for all $\tau \ge \tau_*$, where $\tau_* = 1/(\pi B\epsilon)$. In particular, all the peaks from the grating lobes region will be lowered below the ϵ-level, when $\tau_* \le \tau_{\text{min}}^{\text{gr}}$. This assumption yields that $\tau_* \le \tau_1^{\text{gr_in}}$ and $\tau_* \le \tau_1^{\text{gr_out}}$ or, equivalently, $B/\Delta f_{in} \ge 1/(\pi\epsilon)$ and $B/\Delta f_{out} \ge 1/(\pi\epsilon)$. We note that, in this case, the overlap ratios, $B/\Delta f_{in}$ and $B/\Delta f_{out}$, become large. This leads to significant (and undesirable) reduction of the waveform's total bandwidth B_{out}. So, we eliminate this case from further discussion and set $B/\Delta f_{in} < 1/(\pi\epsilon)$ and $B/\Delta f_{out} < 1/(\pi\epsilon)$.

Finally, we form the set $\Omega_{(n,m)} \subset \mathbb{R}^3$ of quantities $(\Delta f_{in} t_p, B/\Delta f_{in}, \Delta f_{out}/\Delta f_{in})$ satisfying the conditions i)-iv) and perform numerical search for members of $\Omega_{(n,m)}$ that correspond to waveforms producing desired ACF profiles. In our study, we are interested in the waveforms whose ACF exhibit a predetermined (and, generally, different) levels of sidelobes suppression over I_{r} and I_{gr} (we write ϵ_1 and ϵ_2, respectively, for the quantities defining those levels). Therefore, we set the search criteria as fol-

lows:

$$\text{a) } |R_u(\tau)| \le \epsilon_1,\ \tau \in I_{\text{r}};\ \text{b) } |R_u(\tau)| \le \epsilon_2,\ \tau \in I_{\text{gr}}. \quad (14)$$

As the result, we obtain the "output" set $\Omega_{(n,m)}^{(\mu_1,\mu_2)} \subseteq \Omega_{(n,m)}$ consisting of the parameter values of interest. (Here $\mu_i (i = 1, 2)$ represents the desired level of suppression ϵ_i expressed in dB units).

4.2 Numerical Results

In this subsection we demonstrate some results we have obtained while studying two variants of problem (14), corresponding to the ACF peaks suppression over: 1) the grating lobes region only (here we set $\epsilon_1 = 1$), or 2) both regions of interest.

We have conducted the numerical search for the case, when $K = 35$ (then, clearly, $\Lambda = \{(5,7),(7,5)\}$ and we have the sets $\Omega_{(5,7)}$ and $\Omega_{(7,5)}$ of parameter values to search in), under additional assumption that $\Delta f_{in} t_p$ takes on integer values up to 200.

Our analysis of the first variant of problem (14) shows that it is possible to push the peaks of interest down below the level as low as -50 dB. Figure 5 illustrates the ACF of one of the waveforms we have found.

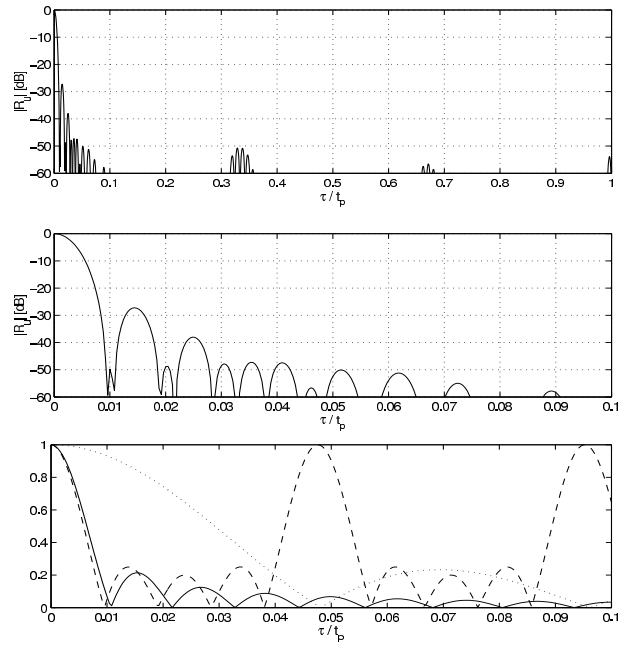

Figure 5. Partial ACF of $u(t)$ with $N = 5, M = 7$, $\Delta f_{in} t_p = 21, \Delta f_{out} t_p = 2.97$, and $B t_p = 94.5$. Top: zoom on the interval $0 \le \tau/t_p \le 1$. Middle: zoom on the interval $0 \le \tau/t_p \le 0.1$. Bottom: the relationship between $|R_1(\tau)|$ (solid), $|R_2(\tau)|$ (dashed), and $|R_3(\tau)|$ (dotted).

Figures 6-9 are related to the case of overall sidelobe suppression. Figure 6 demonstrates the sets $\Omega_{(7,5)}^{(-40)}$ and $\Omega_{(5,7)}^{(-40)}$ (we write $\Omega_{(n,m)}^{(-40)}$ for $\Omega_{(n,m)}^{(-40,-40)}$). As can be seen from the figure, parameters providing the desired threshold level form non-overlapping regions in the $\mathbb{R}^3$. Evidently, one can construct numerous LFM trains satisfying this criteria. A typical ACF for a waveform with the parameters chosen from $\Omega_{(7,5)}^{(-40)}$ is drawn in Figure 7.

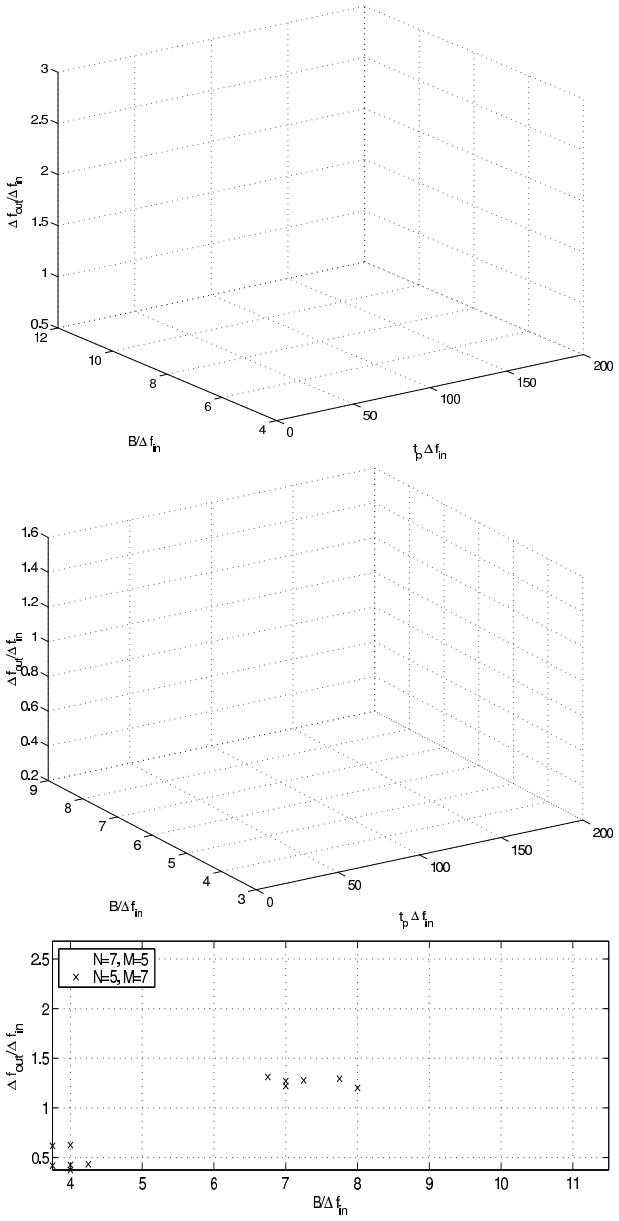

Figure 6. Pictorial representation of $\Omega_{(7,5)}^{(-40)}$ (top) and $\Omega_{(5,7)}^{(-40)}$ (middle). Bottom: The elements of $\Omega_{(7,5)}^{(-40)}$ (denoted by '$\cdot$') and $\Omega_{(5,7)}^{(-40)}$ ('$\times$') for $\Delta f_{in} t_p = 150$.

It appears that the best level of suppression we have been able to find for $K = 35$ is achieved by small number of waveforms associated with $\Omega_{(n,m)}^{(-40,-45)}, (n,m) \in \Lambda$. The ACFs produced by two of them are shown in Figures 8 and 9. The overall level of time sidelobes suppression, for the ACFs depicted, is -41.3dB and -42dB, respectively.

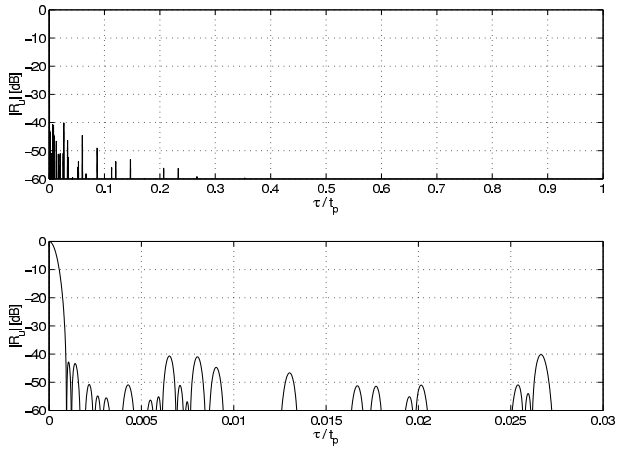

Figure 7. Partial ACF of $u(t)$ with $N = 7, M = 5$, $\Delta f_{in} t_p = 150, \Delta f_{out} t_p = 115.92$, and $Bt_p = 825$. Top: zoom on the interval $0 \leq \tau/t_p \leq 1$. Bottom: zoom on the interval $0 \leq \tau/t_p \leq 0.03$.

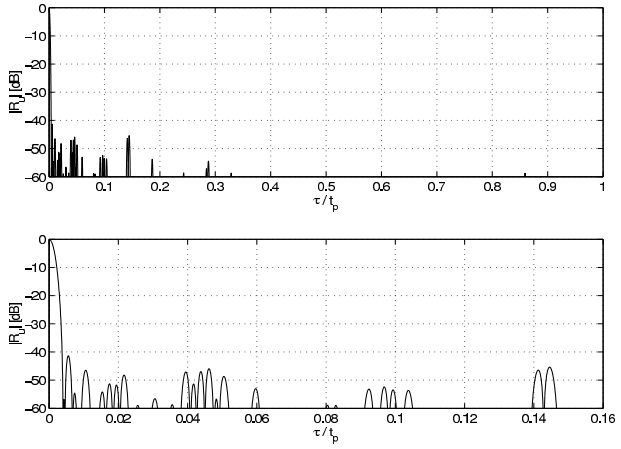

Figure 8. Partial ACF of $u(t)$ with $N = 7, M = 5$, $\Delta f_{in} t_p = 21, \Delta f_{out} t_p = 48.93$, and $Bt_p = 220.5$. Top: zoom on the interval $0 \leq \tau/t_p \leq 1$. Bottom: zoom on the interval $0 \leq \tau/t_p \leq 0.16$.

5 Conclusion

In this paper we have proposed a new family of waveforms that have been designed by a composition of two different stepped-frequency LFM trains with constant frequency steps between the center frequencies of the consecutive pulses. We have showed that, despite of the waveform's complicated structure, its ACF could be written in the closed form. We have used this fact to perform a systematic analysis of the set of the waveform's parameter values, aimed to study their influence on the ACF shape. As the result, we have been able to find a large number of family members producing the ACF with excellent pro-

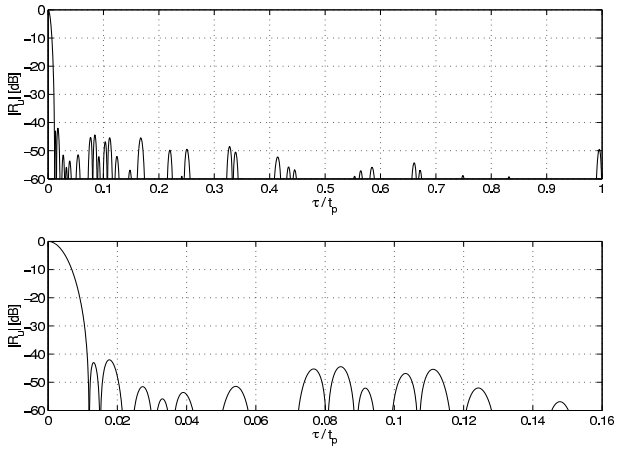

Figure 9. Partial ACF of $u(t)$ with $N = 5, M = 7$, $\Delta f_{in} t_p = 9, \Delta f_{out} t_p = 12.02$, and $Bt_p = 67.5$. Top: zoom on the interval $0 \leq \tau/t_p \leq 1$. Bottom: zoom on the interval $0 \leq \tau/t_p \leq 0.16$.

files. Our analysis, presented, in part, in the paper, clearly reveals that the proposed waveforms have desirable built-in characteristics such as low range sidelobes and low grating lobes, which, along with the other advantages associated with the stepped-frequency waveforms, make them attractive for usage in a high range resolution radar.

Acknowledgements

This work is being sponsored in part by the U.S. Army Research Laboratory and the U.S. Army Research Office under Contract DAAD19-03-1-0329.

References

[1] M.N. Cohen, An overview of high range resolution radar techniques, *Proc. National Telesystems Conf.*, Atlanta, USA, 1991, 107-115.

[2] N. Levanon and E. Mozeson, *Radar Signals* (New York, Wiley, 2004).

[3] D.R. Wehner, *High-Resolution Radar* (Norwood, Artech House, 1987).

[4] D.J. Rabideau, Nonlinear synthetic wideband waveforms, *Proc. IEEE Radar Conf.*, Los Angeles, USA, 2002, 212-219.

[5] N. Levanon and E. Mozeson, Nullifying ACF grating lobes in stepped-frequency train of LFM pulses, *IEEE Trans. on Aerospace and Electronic Systems*, 39(2), 2003, 694-703.

[6] I. Gladkova and D. Chebanov, Suppression of grating lobes in stepped-frequency train, *Proc. IEEE Intern. Radar Conf.*, Arlington, USA, 2005, 371-376.

[7] N. Levanon, Stepped-frequency pulse-train radar signal, *Radar, Sonar, and Navigation*, 149(6), 2002, 297-309.